A Novel Fuzzy Logic Based Sensorless Control for Switched Reluctance Motors Using TI's TMS320F240

Jianrong Bu, Longya Xu

Electrical Engineering Department
The Ohio State University
Columbus, OH43210
email: longya@ee.eng.ohio-state.edu

Abstract: Novel methods for rotor position estimation both at standstill and during running conditions are presented for switched reluctance machine starting free of position sensor and hesitation. By applying a DC pulse to the stator phase windings for a short moment (0.5 ms), the initial rotor position can be accurately detected. Combining the accurate initial rotor position with a novel rotor position estimation algorithm during running, the switched reluctance machine can be started at any initial rotor position without starting hesitation. Critical issues related to optimal model selection as the virtual sensor are discussed in detail. Computer simulation and experimental results are included.

I. Introduction

High performance switched reluctance machine (SRM) drives require accurate rotor position both at standstill and during running conditions. The accurate rotor position is especially significant for wide speed range applications where both magnitude and phase angle of current have to be precisely controlled. Rotor position can be directly measured by a rotor position sensor. However, mounting the rotor position sensor increases the size and cost of the overall system. The rotor position sensor is also a source of unreliability in situations such as high speed, high temperature or where electromagnetic interference presents. Another problem of using rotor position sensor is the rotor starting hesitation associated with the uncertainty of initial rotor position. The rotor starting hesitation is strictly not allowed in high performance servo systems. To remove the rotor position sensor, considerable attention has recently been paid to indirect rotor position estimation [1]-[9]. However, the rotor starting hesitation problem remains in almost all rotor position estimation algorithms thus far.

Critical issues related to high performance rotor position sensorless control of SRMs without starting hesitation are investigated in this paper. Following the detailed description of starting hesitation, model selection for SRM rotor position estimation at standstill and during running conditions is first discussed. Then, novel methods for rotor position estimation both at standstill and during running conditions are presented. Based on the rotor position estimation methods, a reliable starting procedure without rotor starting hesitation is proposed. Computer simulation and experimental results are provided to substantiate the effectiveness of the proposed algorithms. Conclusions are made accordingly.

II. Analysis of SRM Starting Hesitation

The rotor starting hesitation can be understood by examining the following starting process with a rotor position sensor. To ensure the SRM to rotate in a desired direction, the initial rotor position must be known. In a SRM with a rotor position sensor, rather than measuring the initial rotor position, rotor position initialization (or alignment) is done before starting. In this case, the DC bus voltage is applied to a stator phase (for example, Phase A) for a brief moment to pull the rotor to the aligned position with respect to a pair of stator poles as shown in Fig. 1. After the pair of stator and rotor poles are aligned, appropriate starting of the SRM can be launched in the desired rotation direction. For a clockwise rotation, Phase D is excited, otherwise, Phase B. It is clear that during the rotor initialization process, the rotor could move towards the undesired direction, resulting in starting hesitation. The starting hesitation can be found in other cases as well:

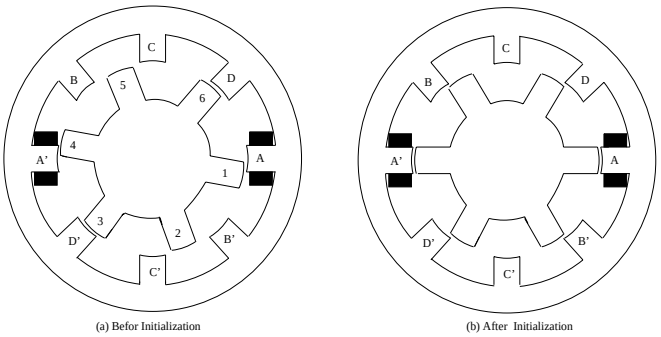

Figure 1: An 8/6 SRM.

- To pull a rotor with a large inertia into alignment with the stator poles, the initialization current generally has to be large. The large current causes the rotor to overshoot and vibrate around the aligned rotor position, which usually takes more than 0.5 seconds resulting in substantial starting hesitation.

- Before the SRM rotor is pulled to the aligned position, the rotor may be in a neutral position. For example, in Fig. 1, the rotor is in a neutral position relative to Phase C. If Phase C is used for initialization, either rotor pole 5 or 6 could be attracted to the aligned rotor position. In the worst case, the rotor may be locked and never be pulled to the aligned rotor position if the SRM is completely symmetrical,

Many technical papers discussing the topic of sensorless control have been published but with no rotor starting hesitation discussed. Similar rotor position initialization process as that in controlling SRM with sensor is applied in most sensorless control algorithms. The sensorless control methods could be based on either chopped current waveforms [1], [2] or diagnostic pulses [7],[8]. Obviously, the chopped current method can not be used to find the initial rotor position at standstill, and hence, to eliminate starting hesitation. On the other hand, by applying diagnostic pulses to a phase winding, the rotor positions at standstill and in running may be estimated. However, the mutual coupling among the phases prevents this method from being effective once the SRM is running at high speeds [9]. An open-loop method can also be used to start a SRM [6]. Assuming that clockwise rotation is desired, the phase excitation sequence should be A-D-C-B-A according to Fig. 1 regardless the initial rotor position. The open-loop method excites the phase windings in the above sequence with the appropriate frequency. After the rotor reaches a threshold rotor speed, the rotor position estimation method then is activated. However, like any open-loop methods, the above method is sensitive to load conditions and unreliable. It can not guarantee the elimination of starting hesitation either.

III. Sensorless Control without Starting Hesitation

A. Model Selection for Rotor Position Estimation

As the first step to develop SRM sensorless control algorithms without starting hesitation, the model selected for rotor position estimation is critically important. The general principles for most SRM rotor position estimation methods are based on the measurement of phase current "i" and flux linkage "λ" (or phase inductance "L"), and the pre-known magnetizing characteristics. That is, at a given instant, if the phase current and flux linkage (or inductance) are known, the rotor position can be uniquely determined from the pre-known magnetizing characteristics. Two types of SRM models are usable for rotor position estimation. The first type describes a SRM in terms of the relationships among phase flux linkage, current and rotor position, and the second type uses phase inductance, current and rotor position. The first type is much preferred because the computation or measurement of flux linkage is more direct and simpler than that of inductance.

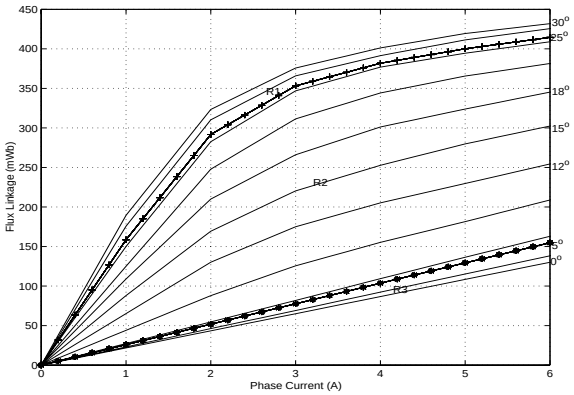

Figure 2: Magnetizing Characteristics of an 8/6 SRM.

Fig. 2 shows the measured relationships among phase flux linkage, current and rotor position for an 8 stator/6 rotor pole (8/6) SRM. In this figure, except for the "*" and "+" curves, the rotor position difference between any two adjacent curves is 3^o. Because the curves are directly measured under the actual operating conditions, all factors including rotor positions, current levels, saturation and mutual coupling are considered naturally. The top and bottom curves in the figure correspond to the magnetizing characteristics at aligned and unaligned rotor positions. If the unaligned rotor position is defined as 0 degrees, the "*" curve corresponds to the magnetizing characteristics at 5^o and the "+" curve at 25^o. According to the "*" and "+" marks, the whole range of magnetizing characteristics of the SRM is divided into three regions; Region R1 above the "+" curve, Region R2 between the "+" and "*" curves, and Region R3 below the "*" curve. From Fig. 2, it can be observed that every pair of values of phase flux linkage and current specifies a unique rotor position. However, utilizing the family of λ-i curves to derive the rotor position, the estimation has very different accuracies in different regions. In Regions R1 and R3, because the adjacent curves are very close to each other, the rotor position estimation accuracy is low, and small errors in flux linkage and/or current measurement can result in a large error in rotor position estimation. In contrast, the rotor position estimation accuracy is high in Region R2, and small errors in flux linkage and/or current only results in a negligible estimation error because for the same

amount of incremental rotor position difference (3^o), the curves are separated widely in the λ-i plane. From the λ-i curves, it is also clear that sufficient current value is needed for accurate rotor position estimation. Therefore, a good estimation method should conduct the rotor position estimation in Region R2 with an adequate phase current.

B. Rotor Position Detection at Standstill

From the discussion in Section II, it is clear that to eliminate starting hesitation, it is necessary to obtain information of the rotor position without initializing and disturbing the rotor at standstill. The method of eliminating starting hesitation presented in this paper is based on the initial rotor position estimation realized in the following steps. 1) Excite all phases for a very short moment (0.5 ms). 2) Find the phase having the largest current. 3) Choose a phase next to the phase having the largest current to be the optimal phase for the rotor position estimation. In theory, the phase either right or left next to the phase with the largest current can be chosen as the optimal phase. To avoid ambiguity, the right phase is always chosen as the optimal phase in this paper. For example, if Phase A has the largest current, Phase B is chosen to be the optimal phase. 4) Compute the flux linkage for the chosen optimal phase. 5) Estimate the initial rotor position from a pre-stored magnetizing characteristics table based on the current and flux linkage of the chosen optimal phase.

The above estimation method has the following salient features:

1. Estimation is done in the high resolution region: Assuming that Phase C has the largest current (hence, Phase C has the minimum inductance, which indicates that the initial rotor position relative to Phase C is very close to the totally unaligned position), then, Phase D will be selected as the optimal phase for initial rotor position estimation according to the proposed algorithm. From Fig. 1, it can be observed that the possible initial rotor position relative to the unaligned rotor position of Phase D will be between 7.5^o and 22.5^o. Thus, the initial rotor relative to the axis of phase D lies in the high position estimation resolution Region R2 as indicated in Fig. 2.

2. Diagnostic signal is sufficient: If Phase C has the largest current, the current in Phase D will be large and sufficient for accurate initial rotor position estimation.

3. Flux linkage computation is simple and accurate: At standstill, the back EMF in any phase winding is zero. So the phase current during the excitation can be determined by the following equation:

$$i(t) = \frac{V}{R}(1 - e^{-\frac{R}{L}t}) \ , \tag{1}$$

where V is the DC bus voltage, R the phase resistance, and L the phase inductance at initial rotor position. If the excitation duration Δt is short (much less than the inverse of time constant R/L), the phase current will increase linearly. Therefore, the flux linkage in Phase D can be calculated by

$$\lambda_D(\Delta t) = \{V - \frac{1}{2}Ri_D(\Delta t)\}\Delta t \ , \tag{2}$$

where i_D is the measured current in Phase D while λ_D is estimated at the end of Δt. Notice that complicated integration for flux linkage computation is not needed here and a single step computation achieves the flux linkage of interests.

It should be pointed out that to obtain accurate initial rotor position, the duration of excitation should be adequate to build up an appropriate amount phase current. However, the duration of excitation should not be too long, or the initial rotor position of the SRM will be disturbed. In this paper, the current from the excitation is about half of the rated current, and the initial rotor position estimation completes in 0.54 ms. No extra hardware is needed to find the initial rotor position.

C. Rotor Position Estimation during Running

With the known initial rotor position, it is straightforward to determine the sequence of phase winding excitation to guarantee the desired rotation direction. An appropriate rotor position estimation method is still needed to properly lock the current duration relative to the rotor position for the smooth rotation thereafter. The rotor position estimation method proposed during running condition is different from the one at standstill and is shown in Fig. 3. Two-level estimation is contained in the proposed algorithm. The first level compares the current in all phase windings and selects the phase having the largest current as the optimal phase. The purpose of this level is to select a suitable phase, so that the rotor position can be estimated in the high resolution Region R2. In the second or a more detailed level, the controller proceeds to find the accurate rotor position based on the flux linkage and current of the selected optimal phase. The flux linkage integration can be implemented either by software or hardware. In this paper, the flux linkage calculation follows the discrete equation,

$$\lambda(k) = \lambda(k-1) + \{V(k-1) - \frac{1}{2}R(i(k-1) + i(k))\}T_s \ , \tag{3}$$

where $\lambda(k-1)$ and $\lambda(k)$ are the flux linkages at sampling instants $(k-1)$ and (k), $i(k-1)$ and $i(k)$ the phase

currents at sampling instants $(k-1)$ and (k), $V(k-1)$ is the command voltage applied to the phase winding at sampling instant $(k-1)$, and T_s the sampling time.

To explain why during running condition, the phase with the largest current is selected as the one for rotor position estimation, Fig. 4 is given which shows the ideal unsaturated inductance profile of an 8/6 SRM in terms of rotor positions. Viewing Fig. 4, it can be noted that the current in the phase with no inductance variation while the rotor is rotating can not generate any torque except for conduction losses. This implies that the phase current should be controlled high in the increasing inductance period and small or zero in the constant inductance period so that high efficiency operation of SRMs is achieved. The increasing inductance period usually starts several degrees after the totally unaligned position and ends several degrees before the totally aligned position. That is, the inductance period corresponds to the high position resolution Region R2. Therefore the phase having the largest current is selected as the optimal phase for rotor position estimation.

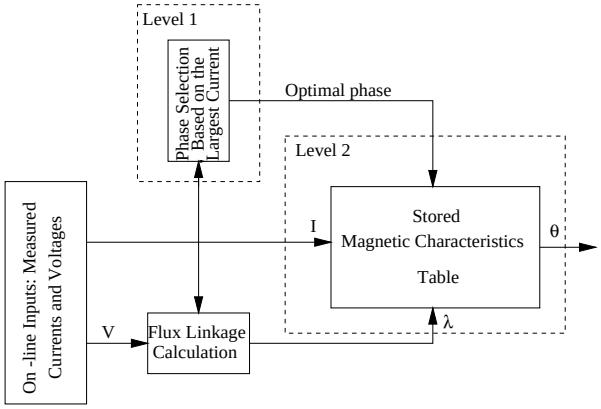

Figure 3: Position Estimation during Running.

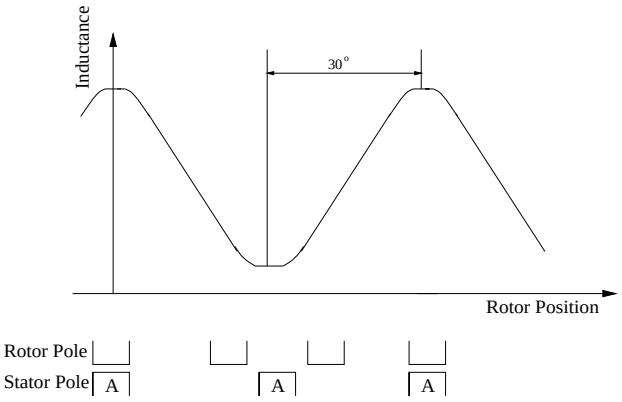

Figure 4: Ideal Inductance Profile of an 8/6 SRM.

D. *Control Flow Chart*

Combining the accurate initial rotor position with the above rotor position estimation algorithm, the SRM can then be reliably started. Because the initial rotor position is accurately found, no rotor position initialization (alignment) is needed, and thus, the starting hesitation is totally eliminated. Fig. 5 summarizes the control algorithms in a flow chart for starting and continuous rotation without using rotor position sensor. In the figure, Blocks 1 through 5 are applied to estimate the initial rotor position as explained in Section III-B. Block 6 determines the phase which should be excite first to ensure the correct rotation. After the initial rotor position is estimated, the selected phase is excited for 200 μs to build up a current before the rotor position estimation algorithm is activated for running condition. This step guarantees an adequate current being established so as to avoid poor estimation accuracy. Blocks 7 through 9 are utilized to estimate the rotor position during running. Based on the estimated rotor position, Block 10 determines the switch status for phase commutation.

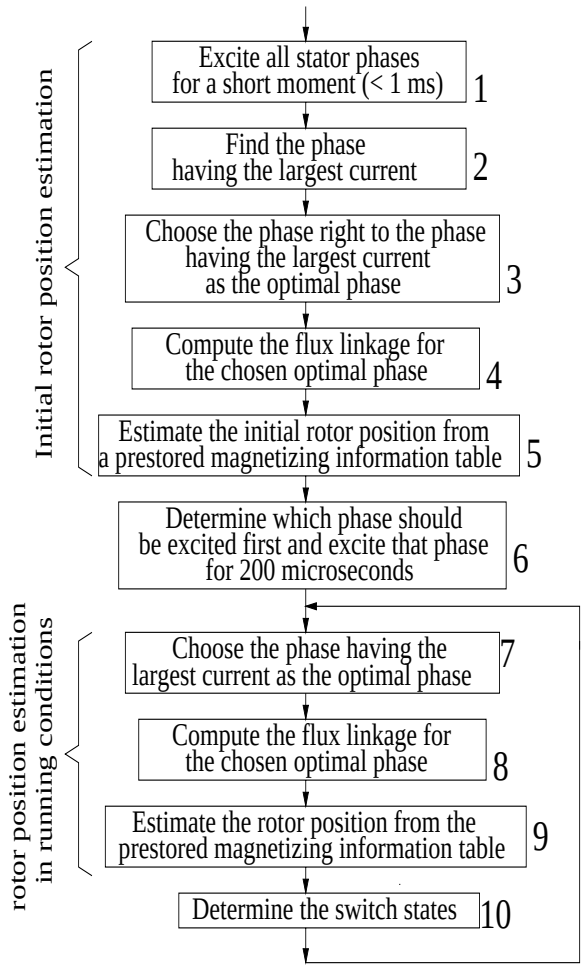

Figure 5: Reliable Sensorless Starting of the SRM without Starting Hesitation.

IV. Computer Simulation and Experimental Results

Computer simulation and experimental investigation were conducted on an 8/6 SRM. The parameters and specifications of the SRM are given below.

$P = 0.5$ HP, $V_{DC} = 160$ V, $n = 3000$ rpm,
$R = 3.5\ \Omega$, $L_u = 21.6$ mH, $L_a = 138.3$ mH.

where L_a and L_u are the phase inductances at aligned and unaligned rotor positions, respectively. The measured magnetizing information of the machine is already shown in Fig. 2. In the following discussion, if not otherwise specified, the rotor position is in mechanical degrees relative to the aligned rotor position of Phase A. Fig. 6 shows the system connection for the SRM control. From the measurement of DC bus voltage and phase currents, the rotor position is estimated by the proposed estimation algorithm. The speed controller compares the command and estimated rotor speeds to generate the command current, turn-on and turn-off angles [10]. Combining all angle and current information, the pulse modulator determines the gating signal to the inverter.

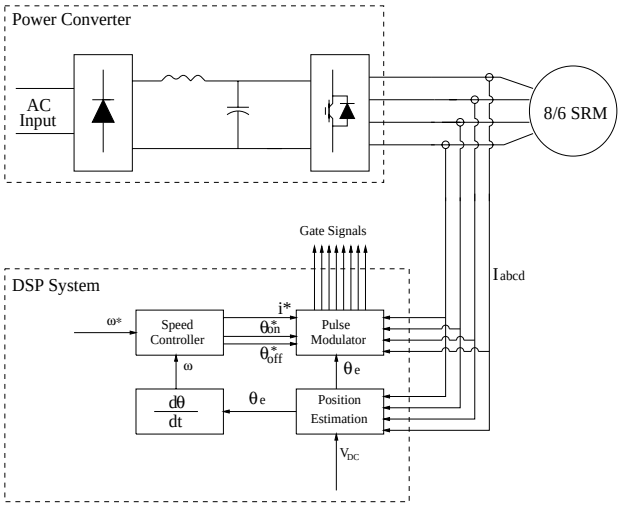

Figure 6: System Connection for the SRM Control.

A. *Computer Simulation Results*

The algorithms for initial rotor position estimation at different initial rotor positions is first verified and the results are given in Fig. 7. The duration of excitation is 0.5 ms. In Fig. 7(a), the actual initial rotor position is arbitrarily given at 15^o. Computer simulation shows that Phase B has the largest current (3.5 A). According to the initial rotor position estimation algorithm, Phase C is selected as the optimal phase. From the current and flux linkage of Phase C, the initial rotor position of 15.4^o is estimated. In Fig. 7(b), the actual initial rotor position is given at 34^o. Computer simulation indicates that Phase A has the largest current (3.1 A) and the optimal phase is B. The initial rotor position is again accurately estimated to be 34.1^o. Fig. 7 also confirms two important assumption of the algorithm: 1) the excitation current will increase linearly if the duration of excitation (0.5 ms) is much less than the inverse of time constant of the stator winding circuit (25.3 s); so the flux linkage can be accurately calculated by the simplified Eq. (2); 2) the optimal phase has a sufficient diagnostic signal. For example, the optimal phase has 0.85 A current in Fig. 7(a) and 0.70 A in Fig. 7(b)

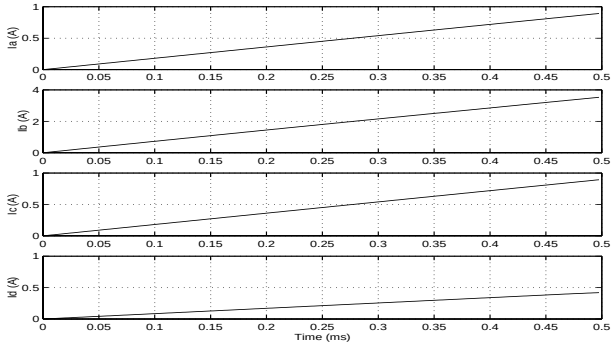

(a) Initial Rotor Position at 15 Degrees

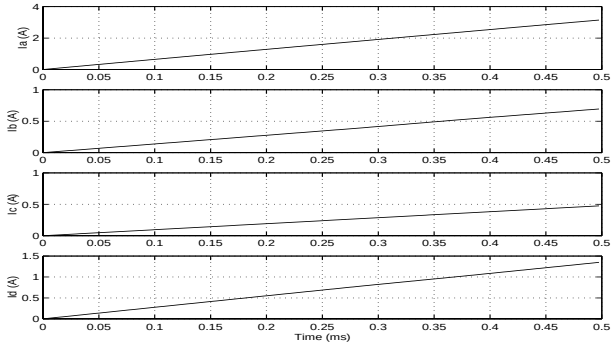

(b) Initial Rotor Position at 34Degrees

Figure 7: Excitation Current for Initial Rotor Position Estimation.

With an arbitrary initial rotor position of 10^o relative to the aligned rotor position of Phase A, Figs. 8 and 9 show the computer simulation results during the starting of the SRM. In Fig. 8, the curves from top to bottom are the actual rotor speed, actual rotor position, estimated rotor position and estimated rotor position error. When the SRM is accelerated from zero to 165 rpm, the estimated rotor position error is between -0.1 and +0.25 mechanical degrees. Fig. 9 shows the corresponding phase currents and the optimal phase for rotor position estimation during the starting process. During starting, the turn-on angle is fixed at 5^o and the turn-off angle at 22^o relative to the totally unaligned rotor position. It can be noted that the optimal phase is Phase C for the ro-

tor position between 10^o and 22^o, Phase B between 20.5^o and 37.2^o, Phase A between 35.5^o and 52.2^o, and Phase D between 51^o and 67.4^o. Referring to Fig. 2, it can be observed that all the rotor position estimation is conducted in the high resolution region, R2, with the largest phase current. So the estimated rotor position has a high accuracy.

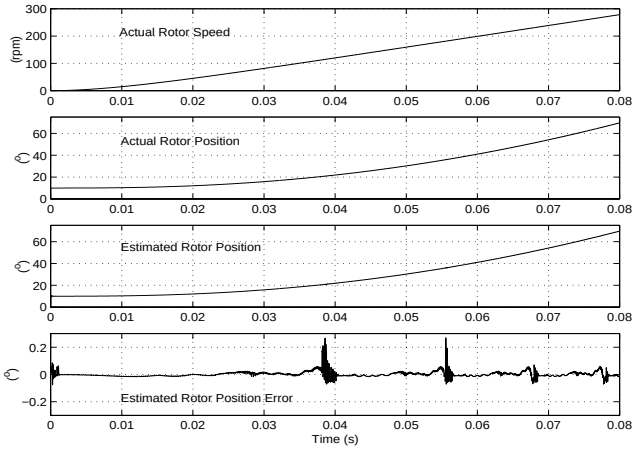

Figure 8: Estimated Rotor Position during Acceleration.

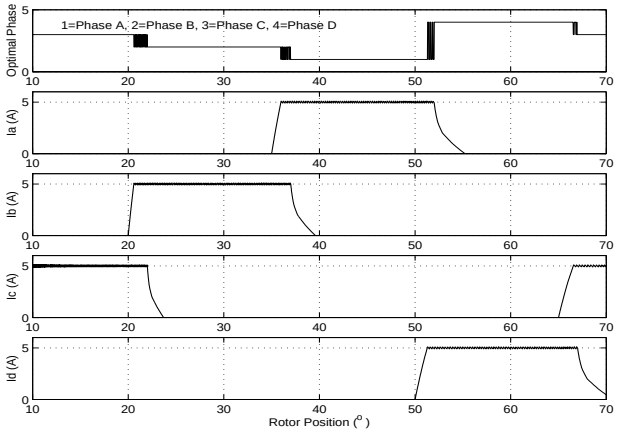

Figure 9: Phase Current during Acceleration.

To verify that the above rotor position estimation method works reliably at high speed, the rotor speed is fixed at 1500 rpm in the computer simulation and the results are shown in Figs. 10 and 11. The turn-on angle is the same as before, but the turn-off angle reduced to 20^o to prevent negative torque production. The rotor position estimation is conducted for the rotor position between 8.0^o and 23^o with respect to the unaligned rotor position of the selected optimal phase. The estimation error is between -0.1 and +0.2 mechanical degrees, as shown in Fig. 10. Comparing Fig. 8 with 10, it can be noted that the estimated rotor position has even higher accuracy at rotor speed of 1500 rpm than that during the starting stage because the rotor position estimation is conducted in a better region in the λ-i plane with the highest resolution. The results also verifies that determining the optimal phase is critical for the high accuracy of rotor position estimation.

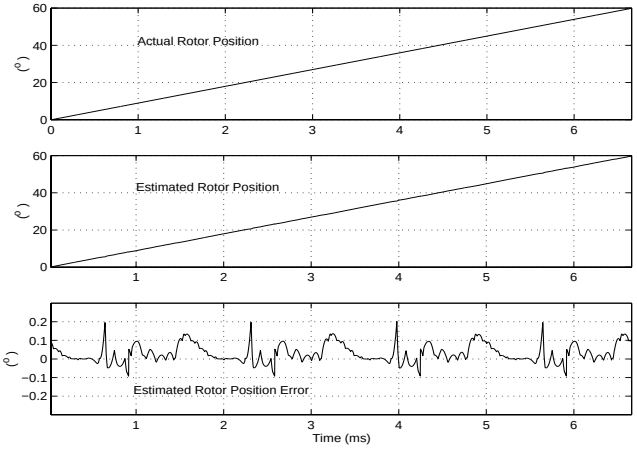

Figure 10: Estimated Rotor Position at Rotor Speed of 1500 rpm.

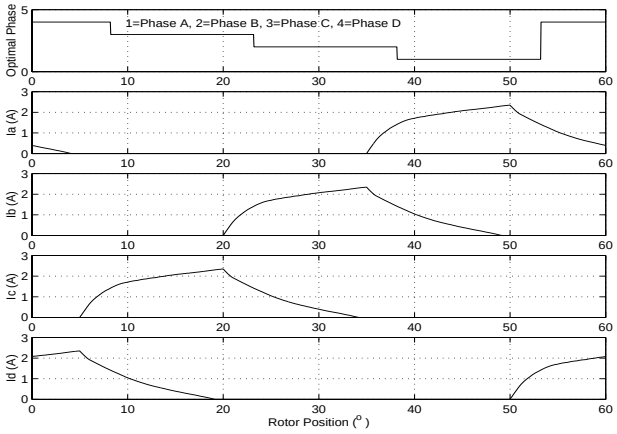

Figure 11: Phase Current at Rotor Speed of 1500 rpm.

B. Experimental Results

Fig. 12 presents the testing results from the simulated 8/6 SRM at different initial rotor positions. The actual initial rotor position is at 12^o in (a), 25^o in (b), and 40^o in (c), respectively. In all figures, the top trace is the rotor speed, the middle the estimated rotor position, and the bottom the measured phase current. The initial excitation and rotor position estimation takes 0.54 ms with the TI TMS320F240 based controller. In 0.35 seconds, the SRM is accelerated to 1200 rpm regardless where the initial rotor position is. The experimental results also

confirm the computer simulation that the starting procedure described in Fig. 5 works well and can start the SRM at any initial rotor position without any starting hesitation. To verify taht the method is not affected by load conditions, in the experiment, we repetitively stalls the SRM by applying a large load torque to the rotor shaft through the dynamometer; nevertheless, the SRM recovers from stalling to the set speed as soon as the stall torque is removed. Fig. 13 shows the starting performance with a heavy load (70 % of rated torque). In the figure, the initial rotor position is arbitrarily set to 20^o degrees. Again, the SRM can be reliably started without starting hesitation.

To verify the effectiveness of the estimation and control algorithms in a more comprehensive operating condition, Fig. 14 shows the 4-Quadrant operation of the SRM with the proposed algorithms. When the rotor speed decelerates from +3000 rpm (or -3000 rpm) to zero, the SRM works in the regenerative mode; and when the rotor speed accelerates from zero to +3000 rpm (or -3000 rpm), the SRM works in the motoring mode. It is evident that the proposed estimation and control algorithms are very effective over a wide range of operating conditions. Fig. 15 shows the details of the rotor position estimation performance during speed zero-crossing. From the top to the bottom, the traces show the rotor speed, estimated rotor position, actual rotor position from optical encoder, and actual phase current. It should be pointed out that the actual rotor position is displayed here only for comparison with the estimated rotor position, and the control is completely based on the estimated rotor position. Comparing the estimated rotor position with the actual rotor position, it can be noted that the rotor position is accurately detected during speed transitions including zero speed. This result fully verifies that the SRM works reliably in 4-Quadrant operation without using rotor position sensor.

V. Conclusions

Novel methods for rotor position estimation both at standstill and during running conditions are presented in the paper. By applying a DC pulse voltage to the stator phase windings for a short moment (0.5 ms), the initial rotor position can be accurately estimated. Combining the accurate initial rotor position with the novel rotor position estimation algorithm during running, the switched reluctance machine can be started at any initial rotor position without starting hesitation. Both computer simulation and experimental results verified that the control algorithm guarantees the SRM a reliable and high performance over a wide range of operation conditions. Future work includes expanding the SRM capabilities of hesitation free and sensorless control to the speed range up to 100,000 rpm.

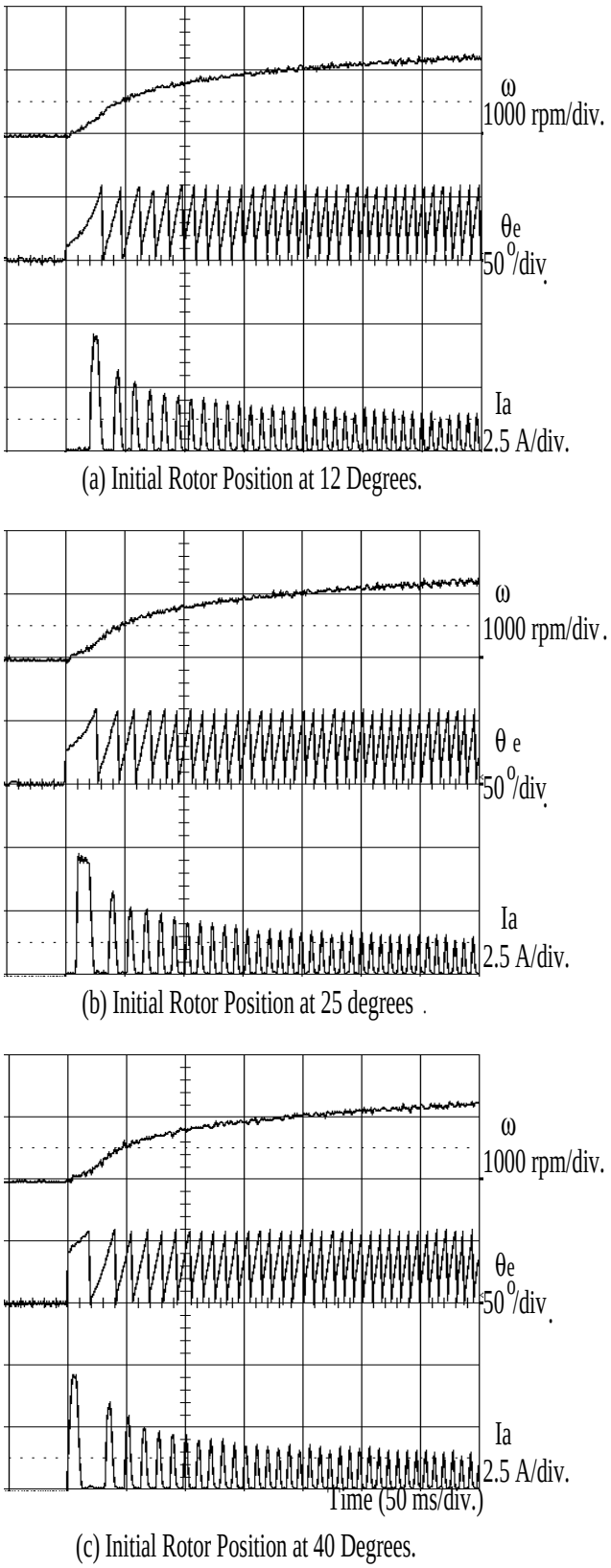

Figure 12: The SRM Starting at Different Initial Rotor Positions.

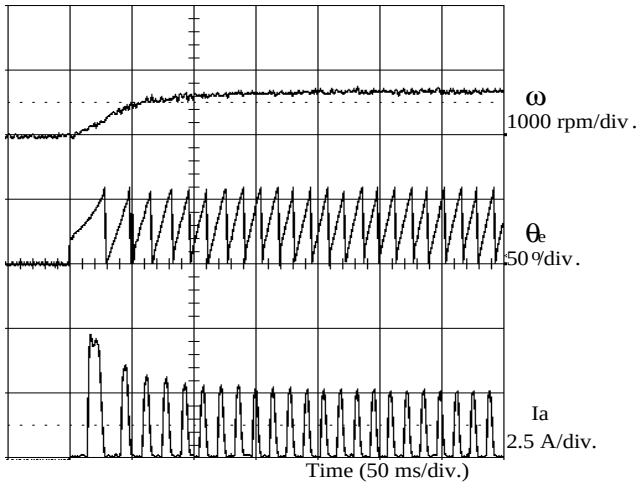

Figure 13: The SRM Starting with 70% of Rated Torque.

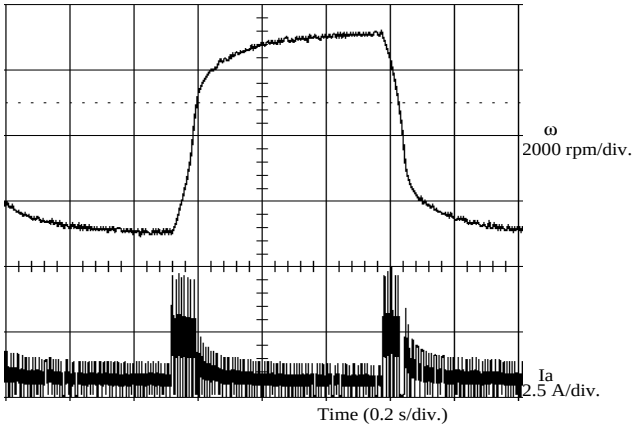

Figure 14: 4-Quadrant Operation without Position Sensor.

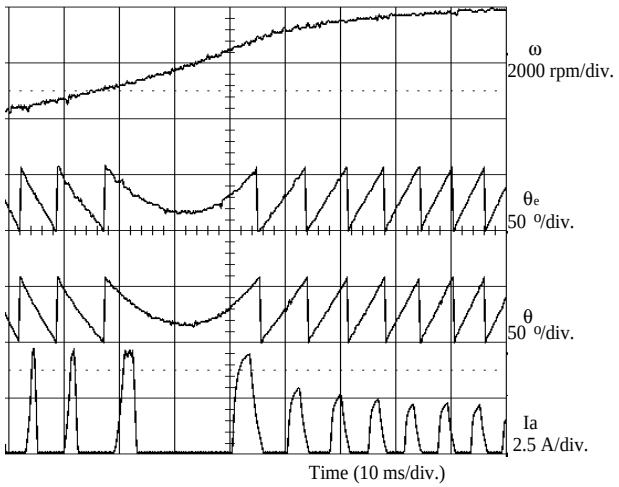

Figure 15: Position Estimation during Rotating Reversing.

VI. Reference

[1] P. P. Acarnley, R. J. Hill and C. W. Hooper, "Detection of Rotor Position in Stepping and Switched Motors by Monitoring of Current Waveforms," IEEE Trans. on Industrial Electronics, Vol. 32, No. 3, pp. 215-222, 1985.

[2] S. K. Panda and G. A. J. Amaratunga, " Waveform Detection Technique for Indirect Rotor-Position Sensing of Switched-Reluctance Motor Drives, Part 1: Analysis," IEE Proceedings B, Vol. 140, No. 1, pp. 80-88, 1993.

[3] W. F. Ray and I. H. Al-Bahadly, "Sensorless Methods for Determining the Rotor Position of Switched Reluctance Motors"', IEE EPE Conference Rec., Brighton, pp. 7-13, 1993.

[4] A. Cheok and N. Ertugral, "A Model Free Fuzzy Logic Based Rotor Position Sensorless Switched Reluctance Motor Drives," IEEE IAS Annual Meeting Rec., San Diego, CA, pp. 76-83, 1996.

[5] L. Xu and J. Bu, "Position Transducerless Control of Switched Reluctance Machine with Minimum Magnetizing Input," IEEE IAS Annual Meeting Rec., New Orleans, LA, pp. 533-539, 1997.

[6] G. Gallegs-Lopez, P. C. Kajr and T. J. E. Miller, "A New Sensorless Method for Switched Reluctance Motor Drives," IEEE IAS Annual Meeting Rec., New Orleans, LA, pp. 564-570, 1997.

[7] M. Ehsani, I. Husain and A. B. Kulkarni, "Elimination of Discrete Position Sensor and Current Sensor in Switched Reluctance Motor Drives," IEEE Trans. on Industry Applications, Vol. 28, No. 1, pp. 128-134, 1992.

[8] M. Ehsani, I. Husain, S. Mahajan and K. R. Ramani, "New Modulation Encoding Techniques for Indirect Rotor Position Sensing in Switched Reluctance Motors," IEEE Trans. on Industry Applications, Vol. 30, No. 1, pp. 85-91, 1994.

[9] W. F. Ray and I. H. Al-Bahadly, "Sensorless Methods for Determining the Rotor Position of Switched Reluctance Motors", IEE Conference Publication, No. 377, Vol. 6, pp. 7-13.

[10] J. Bu, "High Performance Position Sensorless Control of Switched Reluctance Machines over a Wide Speed Range", Ph.D. Dissertation of The Ohio State University, 1998.